Spatial distribution of carbon sources and sinks in Canada's forests

By JING M. CHEN[1,3,*], WEIMIN JU[1], JOSEF CIHLAR[2], DAVID PRICE[5], JANE LIU[1,2], WENJUN CHEN[2], JIANJUN PAN[4], ANDY BLACK[6] and ALAN BARR[3],   [1]*University of Toronto, Toronto, Ontario, Canada;* [2]*Canada Centre for Remote Sensing, Ottawa, Ontario, Canada;* [3]*Meteorological Service of Canada, Saskatoon, Saskatchewan, Canada;* [4]*Nanjing Agricultural University, Nanjing, China;* [5]*Canadian Forest Service, Edmonton, Alberta, Canada;* [6]*University of British Columbia, Vancouver, British Columbia, Canada*

ABSTRACT

Annual spatial distributions of carbon sources and sinks in Canada's forests at 1 km resolution are computed for the period from 1901 to 1998 using ecosystem models that integrate remote sensing images, gridded climate, soils and forest inventory data. GIS-based fire scar maps for most regions of Canada are used to develop a remote sensing algorithm for mapping and dating forest burned areas in the 25 yr prior to 1998. These mapped and dated burned areas are used in combination with inventory data to produce a complete image of forest stand age in 1998. Empirical NPP age relationships were used to simulate the annual variations of forest growth and carbon balance in 1 km pixels, each treated as a homogeneous forest stand. Annual CO_2 flux data from four sites were used for model validation. Averaged over the period 1990–1998, the carbon source and sink map for Canada's forests show the following features: (i) large spatial variations corresponding to the patchiness of recent fire scars and productive forests and (ii) a general south-to-north gradient of decreasing carbon sink strength and increasing source strength. This gradient results mostly from differential effects of temperature increase on growing season length, nutrient mineralization and heterotrophic respiration at different latitudes as well as from uneven nitrogen deposition. The results from the present study are compared with those of two previous studies. The comparison suggests that the overall positive effects of non-disturbance factors (climate, CO_2 and nitrogen) outweighed the effects of increased disturbances in the last two decades, making Canada's forests a carbon sink in the 1980s and 1990s. Comparisons of the modeled results with tower-based eddy covariance measurements of net ecosystem exchange at four forest stands indicate that the sink values from the present study may be underestimated.

1. Introduction

There has been increasing confidence among scientists that the land surface is acting as a carbon sink from the improved estimation of the global carbon budget (Houghton, 1999) and from the partition between the ocean and land in the carbon cycle using inverse methods (Battle et al., 2000; Schimel et al., 2001; Gurney

*Corresponding author address: Department of Geography, University of Toronto, 100 St. George St., Room 5047, Toronto, Ontario, Canada M5S 3G3,
e-mail: chenj@geog.utoronto.ca

et al., 2002). However, the spatial distribution of carbon sources and sinks between and within continents is not yet clear, with different studies indicating different results (Fan et al., 1998; Bousquet et al., 2000; Gurney et al., 2002). Knowledge of the distribution of carbon sources and sinks and their changes over time is critical for understanding the mechanisms controlling the global terrestrial carbon cycle and the sustainability of current carbon sinks. Different ecosystems have different carbon residence times, with northern ecosystems having much longer carbon residence times than those of tropical and temperature ecosystems (Thompson et al., 1996). The relative magnitudes of the carbon

sinks and sources in various ecosystems, therefore, bear significance in estimating the global sink sustainability and in projecting the global atmospheric CO_2 concentration and climate in the near future. More accurate partitioning of sources and sinks among continents and latitudinal bands may be possible in the near future with improved atmospheric inverse modeling and a denser network of atmospheric CO_2 concentration sampling stations. For the present, however, the use of satellite remote sensing and ecosystem models can be the most effective way to quantify detailed spatial distribution patterns. The first purpose of this paper is to demonstrate, through an example of high-resolution Canada-wide spatial modeling, the usefulness of satellite remote sensing data for mapping the distributions of carbon sources and sinks.

Spatially explicit calculations of the carbon cycle would also be a necessary step in increasing the confidence in regional or global carbon balance estimation. Regarding the carbon balance of Canada's forests, there have been two sets of published results. One obtained from forest inventory (Kurz and Apps, 1999) showed that Canada's forests were a carbon source in the last two decades due to increases in the areas disturbed by forest fires and stand-destroying insect attacks. More recently, results obtained from process modeling considered both disturbance and non-disturbance effects (Chen et al., 2000b) and suggested that Canada's forests were a small carbon sink for the period 1980–2000 because the non-disturbance effects, including climate change, nitrogen (N) deposition and CO_2 fertilization, outweighed the effects of increased disturbance. In Chen et al. (2000b), satellite remote sensing was used to obtain the fractions of forest cover types and the mean density for each type, but the carbon cycle estimation was based on forest conditions, climatology and N deposition data averaged across the entire forested area of Canada. The second purpose of the present study is to improve these previous estimates through spatially explicit calculations with the integration of both disturbance and non-disturbance effects.

2. Theories and modeling methodology

2.1. Carbon budget

Net primary productivity (NPP) is a measure of carbon absorption by vegetation per unit time and space, usually expressed in units of g C m^2 yr^{-1} or t C ha^{-1}

yr^{-1}. In process-based estimation, NPP is taken as the difference between the gross primary productivity (GPP), i.e., the gross canopy level photosynthesis, and autotrophic respiration (R_a), i.e.,

$$NPP = GPP - R_a. \tag{1}$$

Net ecosystem productivity (NEP) determines the net exchange of carbon between the land surface (vegetated or non-vegetated) and the atmosphere, without considering the direct carbon release due to disturbance. It is calculated as the difference between NPP and heterotrophic respiration (R_h), i.e.,

$$NEP = NPP - R_h. \tag{2}$$

R_h results from the decomposition of dead organic material in soils, the litter layer above mineral soils and wetland areas. By this definition, when NEP > 0, the land surface is a sink, i.e., it absorbs more carbon than is released. In micrometeorological measurements of carbon fluxes, the term net ecosystem exchange (NEE) is often used (Black et al., 1996). NEE and NEP have the same absolute values but opposite signs, if lateral carbon exchange, e.g., dissolved organic mater in runoff water, is ignored. These definitions of NEE and NEP typically require both an extensive area (such as the footprint of an eddy covariance system) and a significant time period (normally a year or several years).

Net biome productivity (NBP) is used to account for carbon losses due to disturbance at the biome level (Walker and Steffen, 1997). In the study reported here, NBP is estimated for 1 km pixels as:

$$NBP = NEP - D \tag{3}$$

where D is direct carbon release at the time of disturbance. It usually has three components:

$$D = D_{fire} + D_{insect} + D_{log} \tag{4}$$

where D_{fire}, D_{insect} and D_{log} are the amounts of carbon release due to forest fire, insect-induced forest mortality and timber removal, respectively. In our previous work (Chen et al., 2000b), all three components were estimated as the annual national mean values. As spatially explicit data for these three disturbance types are not yet available, we have treated all disturbances as fire, and estimate the C emissions as:

$$D_{fire} = B_f + 0.25B_w + L_{detf} \tag{5}$$

where B_f and B_w are biomass densities of foliage and woody components, respectively, and L_{detf} is the

detritus from foliage. It states that a fire disturbance would release to the atmosphere 100% of the carbon contained in foliage, 25% of that in above-ground woody material and all fine fuel (foliage detritus). Equation (5) is a simplified form of the model by Kasischke et al. (2000). The coefficient of 0.25 for the woody material is used to account for the loss of secondary and primary branches during normal burning and a fraction of boles lost during severe burning (Kasischke et al., 2000). This coefficient of 0.25 for the consumption of woody material is found through adjustment so that the total emission agrees with estimates of Amiro et al. (1999) and Stocks (1991). All components of biomass and detritus vary spatially and are simulated by an ecosystem model named Integrated Terrestrial Ecosystem Carbon model (InTEC), which integrates the effects of disturbance and non-disturbance factors on ecosystem carbon balance (Chen et al., 2000a). The modeled D_{fire} values range from 0 to over 2000 g C m^{-2} with a mean value of about 1210 g C m^{-2}, which is slightly smaller than value of $\sim$1300 g C m^{-2} reported as the average for all forest fires in Canada in the period 1959–1999 (Amiro et al., 2001), but slightly higher than the estimate of $\sim$1200 g C m^{-2} for circumpolar forests by Stocks (1991). The effect of severity of burns on carbon release (Kasischke et al., 2000) has not been considered in this study due to lack of data. After a stand is burned all remaining biomass is assumed to be killed and transferred to the detritus

pools. This includes fine and coarse roots and remaining stems. The decomposition of these increased dead organic matter pools is considered in the subsequent years.

2.2. Model description

The overall methodology of satellite-based carbon balance mapping is summarized in Fig. 1. Satellite remote sensing provides three key inputs: (i) land cover types (Cihlar et al., 1998), (ii) biophysical parameters, such as leaf area index (LAI) (Chen et al., 2002a), and (iii) approximate dates of forest burns (Amiro and Chen, 2003). The information on land cover and LAI, in combination with soil texture and meteorological data, allows us to estimate the spatial distribution of NPP (Liu et al., 1999 and 2002). Date of the last disturbance is also critical for pixel-based simulations of forest carbon dynamics because forest NPP typically varies with stand age. The potential for deriving such information from remote sensing is explored by Amiro et al. (2002) and the remote sensing algorithm derived by them is used in this study. An annual NPP value in each pixel estimated for 1994 in daily steps (Liu et al., 2002, see below) was used to compute NPP for the same pixel retrospectively or progressively in yearly steps for the period 1901–1998 using climate and forest stand age information. The accuracy of calculated NPP time series depends on the NPP and age in
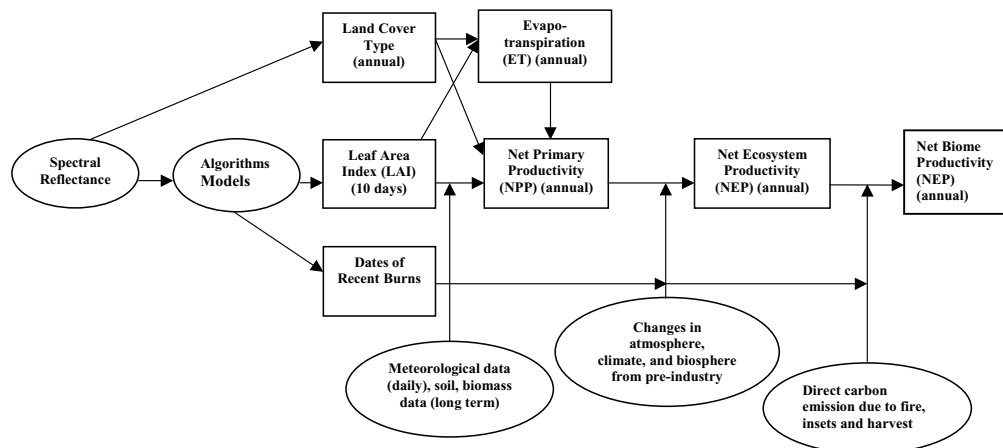
Fig. 1. Major steps in estimating the full carbon cycle in terrestrial ecosystems. Remote sensing provides spectral reflectance data used to obtain the basic state variables (leaf area index, land cover, burn area and date), while the dynamic short-term and long-term processes of the carbon cycle within plants and soils are modeled using the additional inputs of climate, forest stand age from inventory and disturbance data. The end product is an estimate of net biome productivity.

Table 1. *Input datasets, sources, error estimates and impacts of the errors on NEP and NBP in the 1990–1998 period*

Dataset	Sources	Error estimate	Impact on NBP	Impact on NEP
LAI	Chen et al., 2002	25%	0.04%	0.03%
Land cover	Cihlar et al., 1998	20%	2%	0.5%
NPP in 1994	Liu et al., 2002	25%	42–52%	23–28%
ET in 1996	Liu et al., 1999	25%	2.8%	2.6%
Climate	New et al., 1999, 2000	unknown		
Fire polygon	Amiro et al., 2001	<3%	<3%	<1%
Fire scar map from remote sensing	Amiro et al., 2002	±7 yr	16–28%	7–12%
AWC	Shields et al., 1991; Schut et al. 1994	unknown		
Nitrogen deposition	Ro et al., 1995a	10%	6–7%	1–2%
Biomass (inventory)	Penner et al., 1997	25%	2–5%	6–7%
Forest age	Penner et al., 1997	±5 yr	12–22%	5–9%

1994, NPP–age relationship, and physiological functions that described the response of NPP with climate. The most important errors are caused by NPP and age in 1994. The impact of the errors is analyzed in Section 3 (Table 1). Forest stand age for each 1 km pixel was obtained by combining remote sensing methods for the last 25 yr with forest inventory data for stands that were not disturbed in the last 25 yr prior to 1998 image acquisition. Changes in NPP estimated for each pixel over this 98-yr period provides the key information for tracking soil carbon dynamics in the same pixel and quantifying heterotrophic respiration. In this way, the net ecosystem productivity (NEP) can be mapped based on remote sensing. Age–class statistics obtained from ground-based forest inventory data were used to supplement the remote sensing record for the last 25 yr, allowing NBP to be estimated for each pixel.

An ecosystem model, the Boreal Ecosystem Productivity Simulator (BEPS), was developed to simulate NPP in 1994 in daily time steps (Liu et al., 1999; 2002). The Integrated Terrestrial Carbon Cycle Model (InTEC) (Chen et al., 2000a) was modified and adapted for pixel-based long-term simulations of NPP, NEP and NBP. The major components of InTEC model are shown in Fig. 2. InTEC is a combination of: the CENTURY model of soil carbon and nutrient dynamics (Parton et al., 1987; Schimel et al., 1994); Farquhar's leaf biochemical model (Farquhar et al., 1980) for simulating canopy-level annual photosynthesis implemented with a temporal and spatial scaling scheme; and empirical NPP–age relationships (Chen et al., 2002b). It incorporates representations of the known effects on the forest carbon cycle of
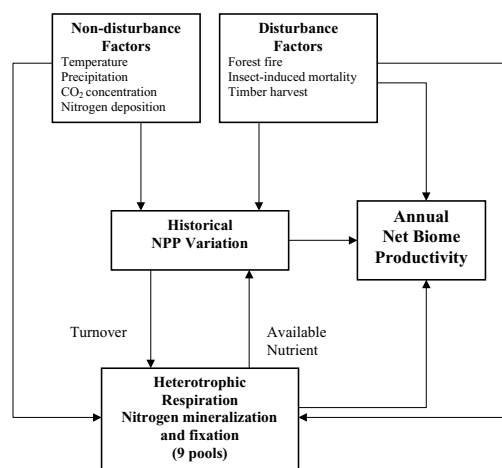
Fig. 2. The major components of the Integrated Terrestrial Ecosystem Carbon Cycle (InTEC) model applied to each 1 km pixel. The historical variation in NPP is central for estimating the amounts of dead organic matter in nine pools (Table 2).

climate change (temperature and precipitation), atmospheric change (CO_2 concentration and nitrogen deposition) and disturbances (fire, insects and harvesting). The interaction between disturbance and non-disturbance factors in carbon cycle processes is also considered in InTEC. Due to the limitations in computing resources, InTEC was applied in annual time steps for all of Canada's forests at 1 km resolution

(approximately 5 million pixels). Coefficients in CEN-TURY were therefore adjusted to represent annual time steps (Table 2). CENTURY was also modified slightly to include more forest detritus pools, i.e., foliage, fine root, coarse root and wood (Chen et al., 2000a).

InTEC employs a constraining strategy to reduce errors in NEP estimates due to uncertainties in NPP and R_h estimates. The strategy is implemented through the assumption of dynamic equilibrium between NPP and R_h in the pre-industrial period (Chen et al., 2000b). In such a way, the carbon balance estimated for recent years results from the accumulated effects of all changes since the pre-industrial period. Errors due to the equilibrium assumption are therefore additive to the total error due to other factors. However, after simulations for 98 yr, which is about twice the mean carbon residence time for boreal ecosystems, any error in the initial years caused by the equilibrium assumption is much reduced for the current years. As the initial error due to deviation from equilibrium would diminish exponentially with time, after two time constants, it would be reduced by a factor of about $e^2 = 8$, i.e., $e^{t/\tau}$ when $t = 2\tau$, where t is time since the assumed equilibrium and τ is the carbon residence time. Such an error estimate shows the importance of performing long-term historical simulations of the forest carbon cycle. To implement InTEC at the pixel level, this assumption is used in two different ways for forest stands of different ages. For stands older than 100 yr, the dynamic equilibrium is assumed to operate before the last disturbance but the net carbon exchange deviates from the neutral condition immediately after the year of disturbance. For stands younger than 100 yr, the equilibrium condition is assumed to exist until 1901, after which the effects of climate change, CO_2 concentration increase and N deposition on the carbon cycle are considered. For a given pixel, stand age increases with time and NPP changes correspondingly with age using a generalized, temperature-dependent empirical NPP–age relationship (see section 3.6). It becomes necessary to find a representative age at which the equilibrium between NPP and R_h before the last disturbance can be assumed to operate. This is particularly important for forest stands younger than 100 yr, because no information is generally available for the stand age at which the last disturbance occurred. For the time span between 1901 and the year of disturbance, therefore, the forest age is assumed to remain unchanged at an "equilibrium age" at which other effects of climate and atmospheric changes are consid-ered. The equilibrium age is defined as the age at which NPP reduces to a level equal or close to heterotrophic respiration. Generally, as a mature forest stand grows older, NPP decreases while heterotrophic respiration may increase slightly due to the accumulation of detritus and soil organic matter from earlier production. As a result of these changes, site-level NEP should generally approach zero or become negative at some stage in the development of the stand. Using InTEC to simulate these dynamics suggests the zero-NEP stage generally occurs in the range from 80 to 150 yr depending on the growth conditions. In cold climates, forests grow slowly and the equilibrium age arrives late. Hence, under conditions of slow growth in northern areas, NEP remains positive at very old ages, and the equilibrium age is found from the rate of change in NEP. Under such conditions, when the change in total carbon (including vegetation and soil carbon) is smaller than a preset threshold value of 1% of NPP, equilibrium is assumed.

In addition to determining the total heterotrophic respiration under the pre-industrial equilibrium conditions for each pixel, it is also necessary to estimate the sizes of various soil carbon pools under equilibrium, because these pools would change in size during a forest life cycle or under changing climate and affect carbon balance in the subsequent non-equilibrium yr. Although this is of second-order importance in terms of NBP when pre-industrial equilibrium is assumed, it is a critical step in validating the components of the model using available data. The sizes of the various pools are found by solving a set of differential equations that consider the interaction among the various pools under the equilibrium condition. The equations contain temperature- and moisture-dependent respiration coefficients for the different pools, corresponding to the general truth that for the same NPP, the substrates in colder regions will contain more carbon than warmer regions. Mathematically, the respiration coefficient for the ith pool (K_i) is calculated as (Parton et al., 1993):

$$K_i = K_{i\_max} f_T(T_s) f_P\left(\frac{P+W}{E}\right)[f_{Li}(L_s)f_{Si}(T_{sc})]$$

(6)

where K_{i_max} is the maximum respiration rate coefficient for the ith pool; T_s, P, W and E are the annual mean soil temperature, precipitation, stored soil water and evapotranspiration, respectively; L_s is the structural lignin content of surface litter and in soils; and T_{sc} represents the silt and clay

fractions of mineral soil. f_T, f_P, f_{Li} and f_{Si} are functions of the designated variable in parentheses. The subscript i in the last two functions indicates that they are pool dependent. L_s is estimated from biomass components using methods and coefficients suggested by Peng et al. (1998), Gholz et al. (2000) and Trofymow et al. (1998). T_{sc} is obtained from the GIS database of Soil Landscapes of Canada (Shields et al., 1991; Schut et al., 1994, see also http://sis.agr.gc.ca/cansis/references/1994ss_a.html). In our pixel-based modeling, the equations used in CENTURY (Parton et al., 1993) were adopted to evaluate the influence of soil moisture, lignin content and soil texture on organic carbon decomposition rates of the various pools.

Under the assumption that decomposition reaches a maximum at 35 °C (Chen et al., 2000a) the temperature response function is

$$f(T_s) = e^{308.56\left(\frac{1}{35+46.02} - \frac{1}{T_s+46.02}\right)}. \tag{7}$$

This equation is reliable for the mean annual temperature $T_s < 35$ °C. All of Canada's forests satisfy this condition.

The function $f[(P + W)/E]$ is an adjustment of heterotrophic respiration for changes in soil water regime (Parton et al., 1993). This adjustment is important for lowland areas, where P is consistently much larger than E, but produces only a second-order effect for about 86% of the forested area in which the fraction of low land area is negligible. A simple approximation to this adjustment was made using data from an evapo-transportaion map of Canada in 1994 calculated using BEPS (Liu et al., 1999) and annual gridded P data.

Methods for estimating the growing season length using the mean spring temperature, the effects of CO_2 and nitrogen fertilization, and nitrogen mineralization and uptake are all reported in Chen et al. (2000a and 2000b).

3. Data sets used

To consider all the major effects of disturbance and non-disturbance factors on carbon balance in each pixel, the following data sets were produced and compiled from various sources. All spatial data were made compatible with remote sensing imagery on a 1 km resolution grid of 5700 × 4800 pixels. All grids use a standard Lambert conformal conic (LCC) projection with 49° and 77° N standard parallels and a 95 °W meridian. All input data are processed into this resolution and projection before or during model execution.

3.1. Leaf area index

Canada-wide LAI maps in 1994 were produced from 10-d cloud-free composite images of the NOAA-11 AVHRR sensor during the growing season (defined as April 11 to October 31, supplemented by 1993 data to replace missing data after September). The composites of AVHRR channels 1 (red) and 2 (NIR) were produced using the maximum NDVI criterion and were corrected for the atmospheric effects using the Simple Model for Atmospheric Correction (Rahman and Dedieu, 1994). After the correction, the radiance data were converted into reflectance and were normalized to a common geometry, i.e., nadir view and 45° solar zenith angle (Cihlar et al., 1997), using a modified Roujean model (Roujean et al., 1992; Chen and Cihlar, 1997). The algorithms for LAI retrieval and the derivation and validation of AVHRR LAI maps are described in Chen et al. (2002a). The accuracy of LAI in individual AVHRR pixels was found to be about 75% in general (in cases of insufficient data for atmospheric correction in far north, the accuracy reduces to 50%), but the accuracy for the average LAI value would increase with increasing area because most errors are random due to unknown mixture ratios of cover types within individual pixels. As the area size increases, the mixture ratio between deciduous and conifer would be less variable.

3.2. Land cover

A land cover map was produced from 20 10-d cloud-free AVHRR composites acquired during the 1995 growing season using methods described by Cihlar et al. (1998). There are 31 cover types in the map, of which 15 are forest cover types. All forest cover types are included in this study. In the long-term simulation of NBP, the cover types are assumed to be unchanged, but disturbances would reset the age to zero while the cover types remain the same.

3.3. Net primary productivity (NPP) and evapotranspiration (ET)

Using the LAI and land cover maps of Canada described above, daily NPP and ET in 1994 were estimated at 1 km resolution using BEPS (Liu et al., 1999; 2002). Gridded daily meteorological data from the National Center of Atmospheric Research and

available soil water holding capacity data from the Soil Landscapes of Canada database (see section 3.8) were used in these calculations.

3.4. GIS-based fire scar data

The Canadian Large-Fire Data Base (LFDB) was compiled from datasets maintained by provincial, territorial and federal agencies (Amiro et al., 2001). The dataset provides polygons mapped in a Geographical Information System (GIS), which delineates the outline of the fire and attribute information, such as fire start date, year of fire, fire number and final area burned. It includes 8880 polygons of fire scars larger than 200 ha distributed across much of the boreal and taiga ecozones, going back as far as 1945 in some areas (Stocks et al., 2002). The LFDB includes fire records for the 1959–1995 period. These fire polygons were co-registered with remote sensing images and used to estimate the forest stand age in pixels that overlap with the polygons. The data-sets were also used to develop the remote sensing algorithm to detect and date fire scars that were not included in LFDB (see section 3.5).

3.5. Satellite-based fire scar area and date

Satellite imagery was used to supplement data from inventory and LFDB to complete a Canada-wide forest stand age map in 1998. Satellite imagery is useful for purposes of extending the fire record from 1995 to 1998 and discovering fire scars that are not included in the LFDB. Fire scar maps for the 25 yr prior to 1998 were produced using data from the VEGETATION sensor onboard the SPOT4 satellite. Nine 10-d cloud-free Canada-wide composites from 1 June to 30 August 1998 were ordered from the VITO center in Belgium. The maximum NDVI criterion was also used in producing the composites from daily cloudy images. The angular normalization scheme developed for AVHRR (Chen and Cihlar, 1997) was applied to the VEGETATION data set. Ratios of shortwave infrared (SWIR) to NIR in these nine images were averaged for each pixel to produce a single ratio image for the mid-summer. The averaging process was necessary as SWIR signals are sensitive to rainfall events. The relationship found by Amiro and Chen (2003) between the mean SWIR/NIR ratio in the summer and the number of yr since the last burn was used to develop an algorithm for mapping the fire scar areas of the individual yr between 1973 to 1998. The r^2 values of the relationship range from 0.57 to 0.80 for 16 of 18 ecoregions.

In the algorithm, the difference between the various types of disturbance, i.e., fires, insect-induced mortality and timber harvest, cannot yet be easily differentiated by remote sensing. We have therefore treated all remotely detected disturbed areas as burned areas. The difference between burned and insect-killed or harvested stands in terms of the carbon cycle is the temporal dynamics of carbon release. Burned stands release about 30% of C in biomass directly to the atmosphere at the time of burning and the rest of biomass is assumed to be killed and transferred to dead organic matter (DOM) pools, while insect-infested and harvested stands transfer part (or, in the case of unsalvaged stands killed by insects) all of biomass material to DOM pools. Our simple treatment of disturbance due to the lack of spatially explicit data for the different types of disturbance will therefore affect the interannual variability of national NBP, but its effect on the decadal average is estimated to be small ($<$10% in NBP) through sensitivity analysis. The dating algorithms have accuracy of $\pm$7 yr for scar ages smaller than 25 yr (Amiro and Chen, 2003), and the total disturbed area in any 5-yr period is within 10% of the total reported by Kurz and Apps (1995).

3.6. NPP–age relationship

Relationships between NPP and stand age were established from analysis of stand yield data for black spruce in Ontario (Chen et al., 2002b). These relationships vary with site conditions quantified using a site index in terms of height above water-logged areas (Fig. 3). For application of the relationships to large areas, a general semi-empirical mathematical function was developed:

$$\text{NPP(age)} = A \left(1 + \frac{b \left(\frac{\text{age}}{c} \right)^d - 1}{\exp \left(\frac{\text{age}}{c} \right)} \right) \qquad (7)$$

where the parameters A, b, c and d are dependent on the site index. In large-area applications of the relationship, however, the site index is replaced with a "dominant factor influencing forest growth", taken as the mean annual air temperature (T_a). The co-registered maps of NPP and T_a in 1994 were used to adjust these parameters in terms of T_a. The corresponding average values of NPP and T_a of each sub-region (100 km × 100 km) were first calculated. The averaged NPP was taken as that at the mean age in the sub-region, which was generally found to be close to the approximate mean forest age of 80 yr. These
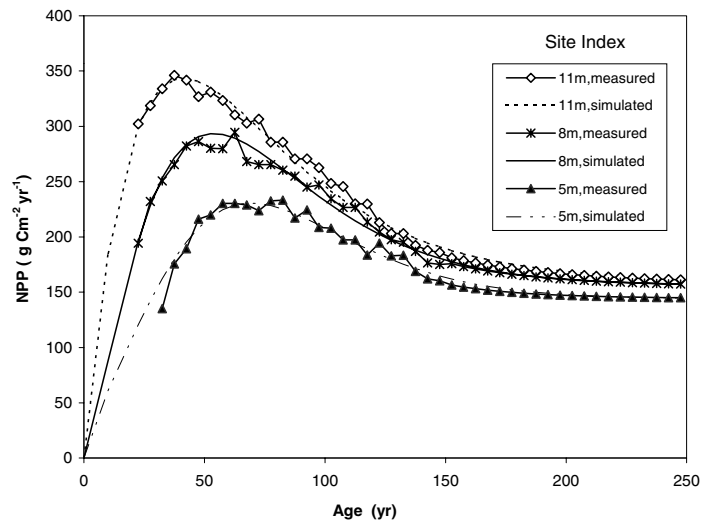
Fig. 3. Simulation of the relationships between NPP and stand age derived from black spruce stand yield data (Chen et al., 2002b) using a semi-empirical function [eq. (7)]. The curves are separated using a site index which is the height in meters above waterlogged areas.

corresponding data for T_a and NPP at a known age then allowed the derivation of the parameters in eq. (7) as functions of T_a. In the Canada-wide application, the NPP–age curve was normalized against the maximum NPP in a forest life cycle, so that the maximum is unity, appearing at different stand ages depending on temperature. After the normalization, all coefficients become sole functions of the mean annual temperature, and a normalized curve is determined when the mean annual temperature is known at each location. The normalized curve was then used for each pixel with the knowledge of age and NPP in 1994, to simulate the historical stand dynamics either under a scenario of no climate and no atmospheric change (baseline case) or using historical climate and atmospheric data (see section 4.4). NPP differs among various forest types in absolute magnitude, while the general shapes of its variation with age are similar. The normalization procedure significantly reduces errors resulting from using the black spruce curves for other species or cover types. The use of a family of curves depending on temperature is a large improvement over a fixed NPP–age relationship used in previous work of Chen et al. (2000b).

3.7. Climate

Monthly data of mean air temperature and precipitation for Canada in the period 1901–1998 were obtained from the 0.5° global data set interpolated by

the UK Climate Research Unit from available station observations using the methods of New et al. (1999; 2000). For annual calculations, the monthly precipitation data were summed, and the monthly temperature data averaged to obtain spring (March–May), growing season (June–August) and the annual means. The total precipitation and average temperature data in 0.5° grid cells were then applied to the 1 km remote sensing images using a bilinear interpolation scheme (Liu et al., 1999).

3.8. Soil texture and carbon

Data on available soil water holding capacity (AWC), total soil DOM, and silt and clay fraction were obtained from the Soil Landscapes of Canada (SLC) database, the best soil database currently available for the country (Shields et al., 1991; Schut et al., 1994, Tarnocai, 1996; Lacelle, 1998). AWC is available in SLC version 1.0 only, with missing values in some areas of the country. To fill the gaps, the relationship with soil texture given by De Jong et al. (1984) was used to estimate AWC from the dominant soil texture in each polygon in the SLC version 2.0. The texture data were complete for all areas of Canada. Data for DOM and silt and clay fraction were obtained directly from SLC version 2.0. To generate these data layers with the same projection and resolution as for other data layers, the original vector data in SLC were mosaicked,

reprojected and rasterized using the ARC/INFO geographic information system.

3.9. Nitrogen deposition

Nitrogen deposition data for Canada's forests during 1983–1994 were obtained from measurements made by the Canadian Air and Precipitation Monitoring Network (CAPMoN) (Ro et al., 1995). By 1990, CAPMoN operated 29 sites across the country, many of which were located in forested areas. Wet deposition rates of NO_x and NH_4^+ were measured at these sites, and dry deposition and droplet deposition rates (i.e., cloud impact on elevated terrain and fog in non-mountainous terrain) were estimated following Shannon and Sisterson (1992). Since 1980, the N deposition rates have been stable in Canada (Ro et al., 1995). Therefore, an average rate for each station was used for the period 1980–1996, while the rates before 1980 are extrapolated by decreasing the rate exponentially toward a background value in 1895 (Dignon and Hameed, 1989). The station data were interpolated and extrapolated to all forested areas in Canada using inverse distance interpolation (Burrough and McDonnell, 1998). As a national average, N deposition was estimated to have increased from 0.05 to 0.25 g N m^{-2} yr^{-1} between 1895 and 1996.

3.10. Inventory

Gridded data of estimated biomass contained in stems, branches and foliage were derived from the Canadian forest biomass inventory of Penner et al. (1997), which was originally compiled from Canada's Forest Inventory (CanFI) 1991 (1994 version) (Lowe et al., 1996). Penner et al. applied previously published regional equations for relationships between standing merchantable wood volume and total aboveground biomass. These data were reported using a GIS polygon coverage of nominal 10 km square cells. The gridded data used here were obtained by allocating the 10 km cell data proportionally to the 1 km pixels on the LCC projection. An inland water mask was overlaid on this 1 km grid to exclude all pixels known to be dominantly water covered (about 10% of the Canadian land surface). The remaining pixels were then aggregated into 10 km grid cells on a regular raster (i.e., quite different from the 10 km polygons used in CanFI). The data used in the present study were of inventoried areas (in hectares) for each of 11 age-classes, in each grid cell.

Based on some local-scale assessments, concerns have been expressed about the reliability of the data contained in the Penner et al. (1997) Canadian forest biomass inventory. These concerns suggest that the inventoried biomass and area data reported for individual 10 km grid cells, particularly in central northern regions, may have considerable errors. However, there is little doubt that at the national scale, the broad distribution of forest biomass attributes provided in this data set is correct. While several initiatives are in progress to develop better national biomass assessments, these data are presently the best available for Canadian forests.

3.11. Tower flux data

Annual net fluxes of CO_2 measured at four forest sites using the eddy correlation method corrected for underestimates of respiratory fluxes on calm nights were compared with model estimates of NEP. These sites included a 73-yr-old aspen site (53.628 °N, 106.198 °W) in the Prince Albert National Park, Saskatchewan (Black et al., 1996), a 123-yr-old black spruce site (55.880 °N, 98.481 °W) near Thompson, Manitoba (Goulden et al., 1998), a 121-year-old black spruce site (53.987 °N, 105.118 °W) near Candle Lake, Saskatchewan (Jarvis et al., 1997; Arain et al., 2002), and a 53-yr-old Douglas-fir (49.850 °N, 125.317 °W), Vancouver Island, BC (Humphreys et al., 2002). All stand ages are reported as of 2001.

All input datasets are summarized in Table 1 with their sources, error estimates and the impacts of these errors on NEP and NBP in the 1990–1998 period. The impact assessment was done by executing InTEC for all forest pixels with an error treated as a constant fraction of change in the tested parameter. The direct effect of errors in LAI on NEP is small through small changes in the C/N ratio in leaves, but errors in LAI are the main cause of the errors in NPP. The impact of NPP errors on NEP has about the same relative magnitudes as the NPP errors because of the use of the assumption of the dynamic equilibrium in the pre-industrial period (Chen et al., 2000a). The impacts on NBP have relatively larger magnitudes than those on NEP because the absolute value of NBP is smaller than NEP for the period. Errors in forest fire polygon, forest age maps and nitrogen deposition all have considerable effects on NEP and NBP. The impacts of errors in land cover on NEP and NBP are complex but are estimated simply here by randomly replacing 20% of conifer pixels with deciduous pixels. The impacts appear to be very small

(1–2%) under the equilibrium assumption. As the two forest types have the largest difference in NPP, the impact estimate caps the entire range of impacts of errors in other cover types.

4. Results and discussion

For the purpose of computing the spatial distribution of NBP, several intermediate products were first produced from the available input data. These products included a map of mean forest stand age in 1998, maps of modeled aboveground and belowground biomass, and a map of modeled total soil dead organic matter (DOM). The stand age map was the essential input to the model for spatially explicit calculations of NEP and NBP, while the biomass and DOM maps provided additional information for model parameterization and constraint. Model simulations of the historical changes in the carbon balance for individual pixels were compared with measured annual total NEE in recent yr at four tower flux sites. Finally, the computed mean annual NBP values during 1901–1998 for Canada's forests are compared with previous studies.

4.1. Forest stand age map of Canada

A map of forest stand age for 1998 was created using the combined information from forest inventory, fire polygon data and remote sensing. Forest inventory was available as gridded data at 10 km resolution (derived from Penner et al., 1997), with the forested area-fractions provided for various age classes (0–20, 21–40, 41–60, 61–80, 81–100, 101–120, 121–140, 141–160 and older). The inventory was compiled in 1991 and 1994 with the most recent data in the late 1980s, and is therefore outdated for carbon modeling for recent decades. The inventory only includes the commercial forests and has no data for northern boreal regions, which occupies about 50% of total Canada's forested area. Fire polygons in the LFDB provided data the northern boreal regions, but only included large fires in the period from 1959 to 1995. For some provinces and territories, the polygon data records were only about 20 yr. Remote sensing imagery was used to fill in the data gaps in both space and time. Annual forest burned area maps in the yr between 1973 and 1998 were constructed using the fire scar dating algorithm developed by Amiro et al. (2002). These maps were then used to replace the age data in the gridded inventory data while the older age classes in the inventory are unchanged, i.e., we as-

sumed that the inventory age-class data were correct for all grid cells that were not disturbed after 1973. In the combination of these three types of data, a 10 km × 10 km grid cell in the forest inventory was divided into 100 pixels at 1 km resolution. Pixels of different age classes were randomly distributed within the grid cell and were replaced by fire polygons of known dates or by recent fire scars if detected by remote sensing. For simplicity, forest regrowth is assumed to start immediately after disturbance, so the age of forest in a burned area is assumed to equal the time since the date the fire scar was detected by remote sensing. For non-commercial forests, areas with fire scars younger than 25 yr were considered to be reliable, and the other areas are randomly assigned an age in the range from 26 to 110 yr, based on the area fractions in each age class reported for the inventoried regions. Figure 4 shows the Canada-wide distribution of forest stand age. Many recent fires occurred on the Canadian shield in the provinces of Alberta, Saskatchewan and Manitoba. In northern Ontario and Quebec, considerable areas burned in the last two decades were also detected. Forests in British Columbia are mostly older than 100 yr, with some scattered small disturbed areas detected. These spatial distribution patterns of forest stand age have pronounced effects on the spatial distribution of NBP. The use of remote sensing data for recently burned areas has improved the spatial and temporal coverage of the gridded forest inventory data. Due to a lack of more detailed spatial data, this Canada-wide stand age map represents the best of currently available data, although it is likely that further improvements will occur as more remote sensing data and ground-based inventory data become available in the near future.

4.2. Comparison of modeled dead organic matter distribution with Soil Landscape of Canada

Total soil dead organic matter (DOM), including detritus and soil organic carbon (SOC), was modeled pixel-by-pixel based on the modeled NPP history, vegetation carbon turnover rates to detritus, and decomposition rates of various SOC pools. To test the reliability of the calculated heterotrophic respiration, the modeled DOM map was compared with a GIS polygon map of the Soil Landscapes of Canada (SLC, Schut et al., 1994). DOM in wetland polygons identified in SLC is excluded from the comparison because In-TEC does not simulate anaerobic decomposition processes. The outcome of the comparison is summarized
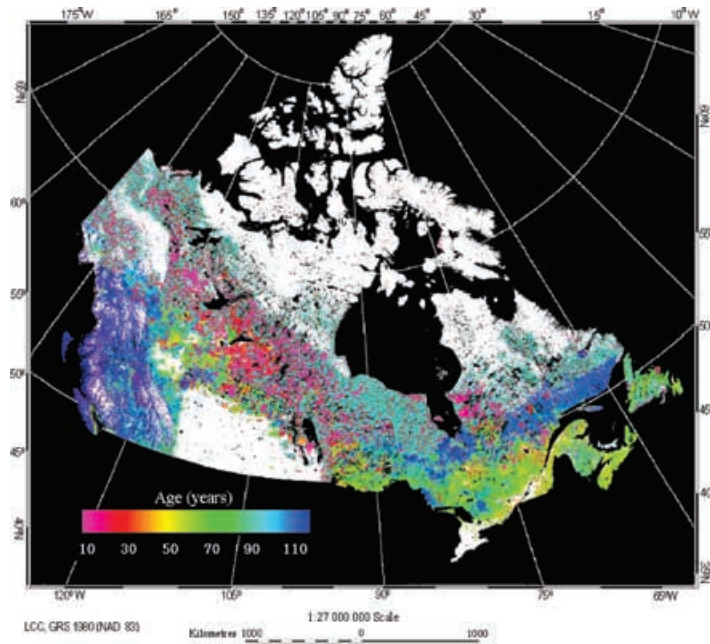
Fig. 4. The distribution of forest stand age derived using a combination of available forest inventory data gridded at 10 km resolution, fire polygons in the period 1959–1995, and remote sensing for the last 25 yr at 1 km resolution.
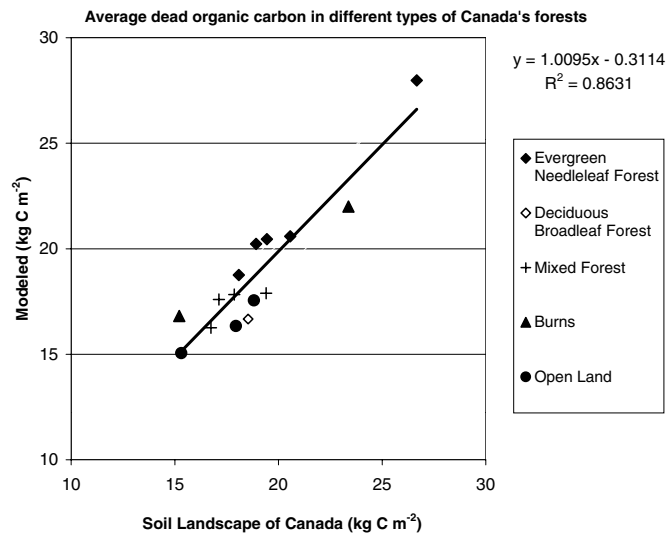
Fig. 5. Comparison of modeled soil dead organic matter with data available from the Soil Landscapes of Canada database for all 15 forest cover types in five groups.

in Fig. 5, with the results grouped into several major forest cover types. The modeled DOM distribution captures the general spatial variation patterns reported in the SLC database. In terms of the mean DOM density for the 15 forest cover types, the model achieved 86% of the variance among the cover types. As NPP and heterotrophic respiration were assumed to be in equilibrium before 1901 or before the last disturbance

Table 2. *Carbon allocation coefficients, turnover rates and decomposition rates of the vegetation and soil carbon components*[a]

| Symbol | Description | Mean cover type | | | | Unit |
		Conifer	Deciduous	Mixed forest	Open land	
Vegetation carbon						
f_w	NPP allocation coefficient to wood	0.3010	0.4624	0.3817	0.3817	Unitless
f_{cr}	NPP allocation coefficient to coarse root	0.1483	0.1190	0.1536	0.1536	Unitless
f_l	NPP allocation coefficient to leaf	0.2128	0.2226	0.2077	0.2077	Unitless
f_{fr}	NPP allocation coefficient to fine root	0.3479	0.1960	0.2570	0.2570	Unitless
K_w	Wood turnover rate	0.0279	0.0288	0.0279	0.0139	yr^{-1}
K_{cr}	Coarse root turnover rate	0.0269	0.0448	0.0268	0.0268	yr^{-1}
K_l	Leaf turnover rate	0.1925	1.0000	0.3945	0.3945	yr^{-1}
K_{fr}	Fine root turnover rate	0.5948	0.5948	0.5948	0.3000	yr^{-1}
Soil carbon						
K_{ssl}	Surface structural leaf litter decomposition rate			$3.9L_cA$		yr^{-1}
K_{sml}	Surface metabolic leaf litter decomposition rate			$14.8A$		yr^{-1}
K_{fsl}	Soil structural litter decomposition rate			$4.8L_cA$		yr^{-1}
K_{fml}	Soil metabolic litter decomposition rate			$18.5A$		yr^{-1}
K_w	Woody litter decomposition rate			$2.88L_cA$		yr^{-1}
K_{sm}	Surface microbe decomposition rate			$6.0A$		yr^{-1}
K_m	Soil microbe decomposition rate			$7.3AT_m$		yr^{-1}
K_s	Slow carbon decomposition rate			$0.2A$		yr^{-1}
K_p	Passive carbon decomposition rate			$0.0045A$		yr^{-1}

[a]A is the combined abiotic impact of soil moisture and soil temperature on the decomposition rate, based on Century model and its adaptation to annual step calculations (Chen et al., 2000a). L_c quantifies the impact of lignin content of structural materials on decomposition. T_m is the effect of soil texture on soil microbe carbon decomposition. Corresponding to Eq. 6, $L_c = f_{Li}(L_s)$, $A = f_T(T_S)f(\frac{P+W}{E})$ and $T_m = f_{Si}(T_{sc})$.

for forests older than 100 yr, any errors in the soil carbon calculation should have only second-order effects on the final NBP estimate. This is because biases in the modeled soil carbon are compensated by the adjustments to the decomposition coefficients of the various pools. As soil carbon estimation and validation is the most difficult part of the terrestrial carbon cycle modeling, the close agreement between the modeled DOM and the available data for all forest cover types in all regions of Canada indicates that the model is well constrained and the model parameterization scheme is effective.

4.3. Comparison of modeled biomass distribution with forest inventory data

Forest biomass in each pixel is also calculated as the accumulated carbon in stems, roots and foliage since the last disturbance. The total C accumulation in vegetation depends on the NPP history, coefficients of C allocation to the various vegetation components, and turnover rates of these components. The use of forest inventory of aboveground biomass allowed us to check

whether these allocation coefficients were reasonable for the various cover types. The final coefficients for the major forest cover types are also given in Table 2. Figure 6 shows the comparison of the modeled C in aboveground biomass with the forest inventory data. Modeled aboveground biomass values for mixed and deciduous forest types are about 30% larger than the inventory data. This may indicate that the allocation of NPP to wood, shown in Table 2, is too large, although the coefficient we used is within one standard deviation of the ground measurement at an aspen site (Gower et al., 1997). The model values of aboveground biomass in sparse forests are considerably smaller than those in the inventory, but the inventory data for this cover type are insufficient and therefore may not be reliable. The best agreement between modeled and inventory values was obtained for conifer forests, which occupy about 53% of Canada's forested areas. Inaccuracies in aboveground biomass estimation have the second-order importance in NBP estimation under the pre-industrial equilibrium assumption (see Table 1), because NBP is driven mainly by changes in carbon storage resulting from disturbance, DOM

Average aboveground biomass carbon in different types of Canada's forests
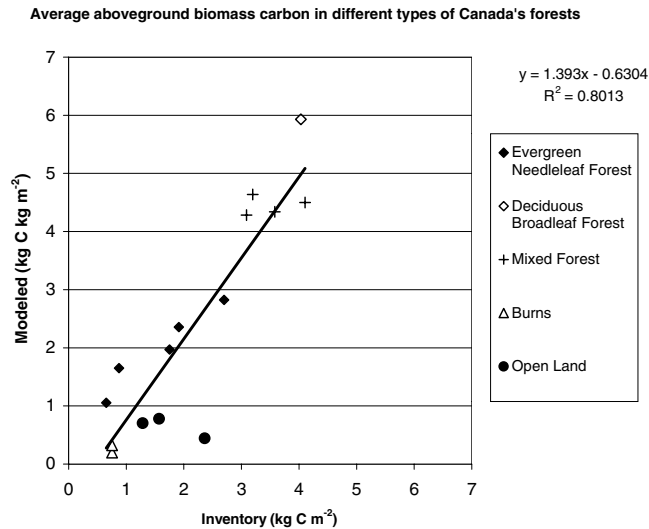
Fig. 6. Comparison of modeled aboveground biomass with data from forest inventories representing 15 major forest cover types across Canada. The major forest types were grouped into the five classes identified in the legend.

accumulation and nutrient cycling. Clearly, significant improvements can still be made in the relative allocations to aboveground and belowground biomass components once more field data become available.

4.4. Validation of NEP results using tower flux data

Net CO_2 exchanges measured using eddy covariance systems mounted on micrometeorological towers provide independent data for checking modeled NEP. Modeled C dynamics in the four pixels containing the tower flux sites also provide an opportunity to interpret the measured flux from the historical perspective based on stand dynamics. The model is used to estimate, at each site, the individual and combined effects on the carbon balance of various factors including climate change, N deposition and CO_2 fertilization. The results are summarized in Figs. 7a–d. In each of these figures, three sets of modeled results are presented. One is the baseline when climate (temperature and precipitation) and atmospheric compositions (N and CO_2) are assumed to be unchanged for the entire modeling period, while the forest was allowed to become progressively older. The second set of simulations is made when historical climate data interpolated to the tower locations were used but changes in atmospheric composition were ignored. The third set accounted for all environmental factors including climate and atmospheric changes. In the cases of stands younger than

100 yr (Figs. 7a and b), modelled NEP was zero for the period prior to the last disturbance in the baseline simulations, i.e., the forest remained in dynamic equilibrium throughout the period before the last disturbance. This is achieved using the concept of equilibrium age described in section 2 to ensure that the model is properly constrained. In the year of disturbance, a large amount of carbon is released directly (not shown in the figures due to the large scales). Following the results of Amiro et al. (2000), the forest regrowth is assumed to start immediately after disturbance. In the early yr of regrowth, heterotrophic respiration exceeds NPP, resulting in negative NEP, i.e., the system is losing carbon to the atmosphere. As NPP increases in the subsequent years, NEP becomes positive and reaches a maximum. Thereafter, the NPP decreases with age, and as does NEP.

In general, modeled NEP agreed with measured values in magnitude, but in some cases the model underestimates the measured values. The largest difference was for the Douglas fir stand in BC (Fig. 7a). The stand was fertilized by air in 1995 with about 200 kg N ha^{-1}, and this local fertilization effect has not yet been included in the model simulation. In the InTEC model, an absorption of 30 kg N ha^{-1} yr^{-1} by the stand can increase NEP by about 2000 kg C ha^{-1} yr^{-1} or 200 g C m^{-2} yr^{-1}. For the 73-yr-old aspen stand in Saskatchewan (Fig. 7b), modeled NEP values agree with measurements in some years but are smaller than

(a)

Temporal variation of NEP in 53 year old Donglas-fir stand
BC (49.850^{0}N, 125.317^{0}W)

(b)

Temporal Variation of NEP in 73 year old aspen stand
Saskatchewan (53.628^{0}N, 106.198^0 W)
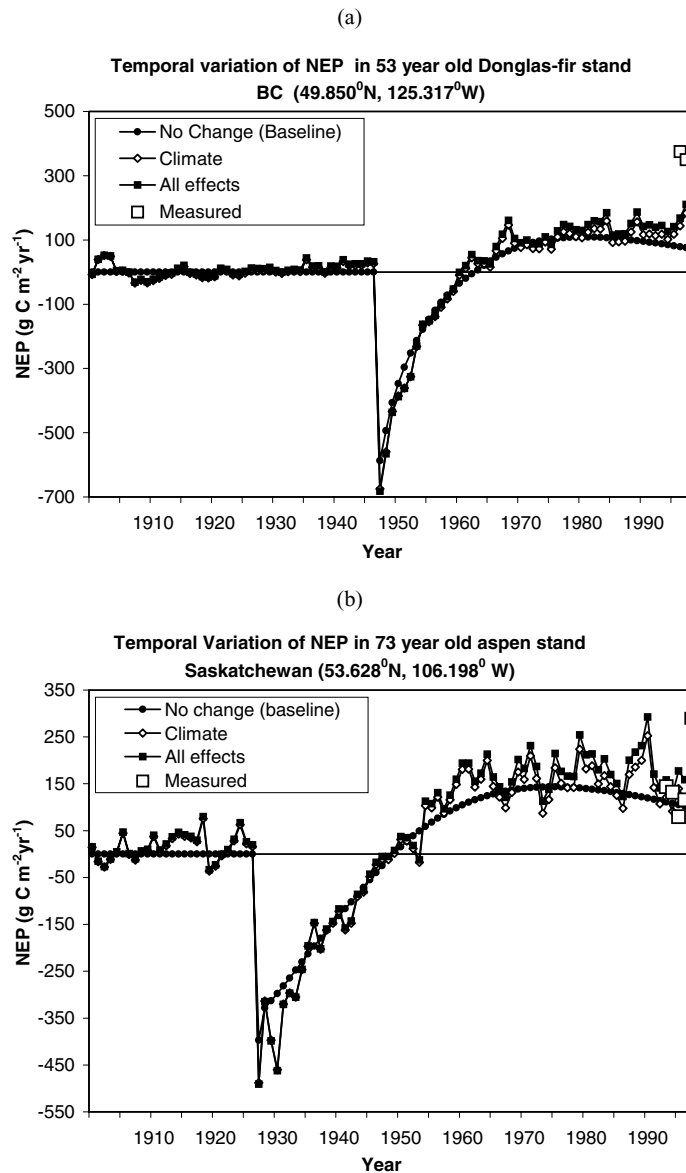
Fig. 7. Interpretation of CO_2 flux measurements in recent years from the historical change perspective based on stand dynamics as affected by changes in age, climate and CO_2 and nitrogen deposition (last two factors are included in "All effects"). The "baseline" case only includes changes in age. (a) 53-yr-old Douglas fir stand; (b) 77-yr-old aspen stand; (c) 121-yr-old black spruce stand; and (d) 123-yr-old black spruce stand.

measured values in most years, indicating a possible negative bias of the model. The results for the two mature black spruce stands (Figs. 7c and d) are similar. In the 121-yr-old stand in Saskatchewan, the modeled value for the year 1994 was smaller than the measured value in the same year. In the 123-yr-old stand in Manitoba, the overall magnitudes of modeled and measured NEP agree in the period 1994–1997,

(c)

Temporal variation of NEP in 121 year old black spruce stand
Saskatchewan (53.987^{0}0 N, 105.118^0 W)

(d)

Temporal Variation of NEP in 123 year old black spruce stand
Manitoba (55.880^0 N, 98.481^{0}W)
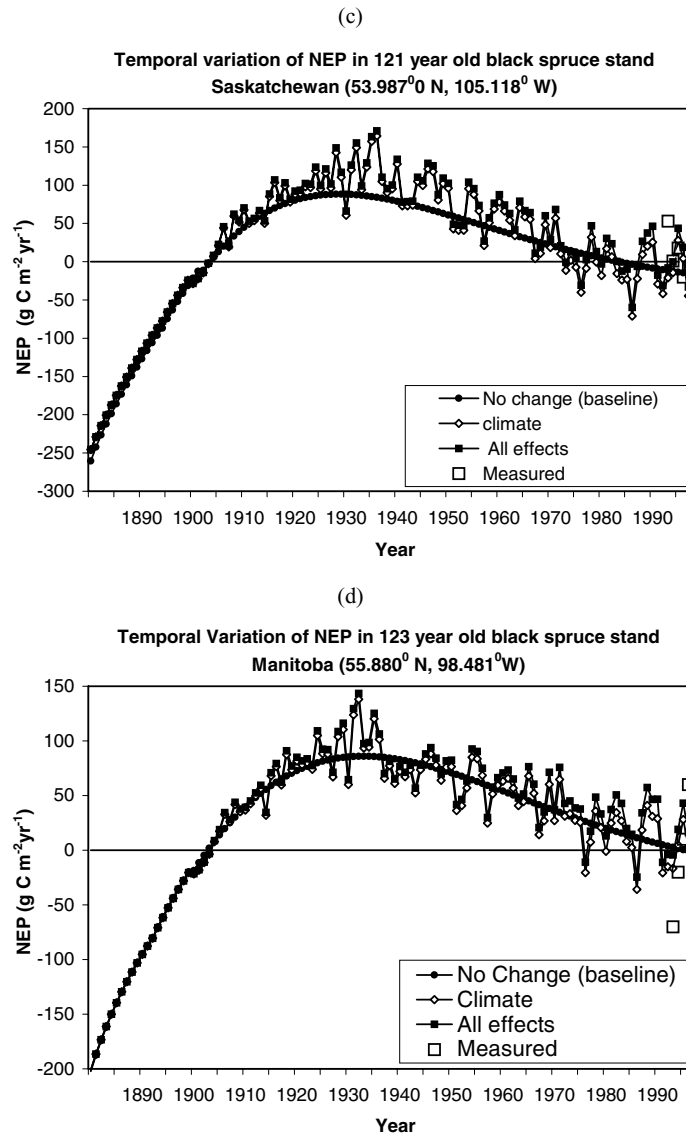
Fig. 7. (cont'd).

although the interannual variations are different between modeled and measured results. Two points can be made from these comparisons: (1) the model tends to underestimate NEP at these tower flux sites, implying that the simulated national NBP statistics shown in section 4.5 below may be slightly underestimated; and (2) the annual time step used for the NEP calculations may be too coarse to simulate inter-annual variability at given sites because it cannot capture well the seasonal variation patterns. In our annual time step Canada-wide pixel-base simulations, the first-order seasonal variability has been considered through the use of spring and growing season temperatures in addition to the annual mean temperature. However, we believe that large improvements in inter-annual variability can be gained by weekly or monthly time step simulations when the computational limitation is reduced in the near future.
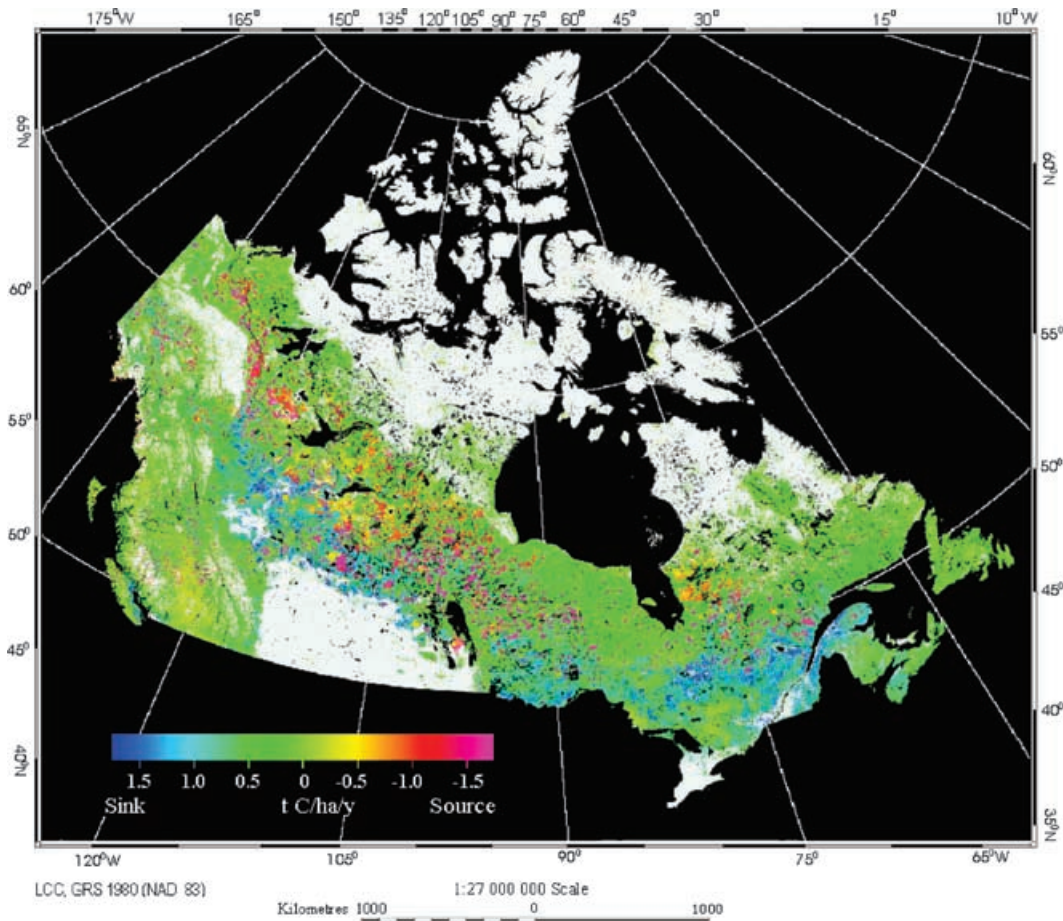
Fig. 8. Carbon source and sink distribution in Canada's forests for the period 1990–1998, in terms of net biome productivity, which includes carbon absorption by vegetation, releases of carbon from soils due to decomposition of dead organic matter and direct releases of carbon during disturbance. The white colour indicates non-forested area.

4.5. Carbon source and sink map in Canada's forests

Canada-wide maps of annual forest NBP were estimated at 1 km resolution for the period 1901–1998. Spatially explicit inputs to the calculation included maps of NPP and ET in 1994, land cover in 1995, the mean seasonal LAI in 1994, forest stand age in 1998, and gridded climate data for 1901–1998, spatially interpolated and temporally extrapolated N deposition in the period between 1901–1998, and gridded available soil water holding capacity. With these inputs, the model was used to generate an NBP map for each simulation year. Interannual variability was

large in various regions. Figure 8 shows a map of NBP expressed as the mean for the period from 1990 to 1998. With the exception of British Columbia (BC), the NBP map is characterized by: (i) the large spatial variations corresponding to the patchiness of fire scar ages and productive forests, and (ii) a general south-to-north gradient of decreasing carbon sink strength and increasing source strength, which is the most apparent in central and eastern Canada. This gradient results mostly from differential effects of temperature increase on growing season length, nutrient mineralization and heterotrophic respiration at different latitudes as well as from uneven nitrogen deposition. In the province of BC, where forests are relatively old,

the forests are near neutral in terms of carbon balance. In BC, nitrogen deposition and CO_2 fertilization have only small but positive effects on NPP. According to the interpolated climate record, the average growing season length increased by about 6–7 d over the last century. These positive effects are balanced by the increase in soil respiration and reduced growth at old ages in BC.

4.6. Comparison with previous results

New insights into Canada's forest carbon cycle emerge when results from three national-scale studies are compared (Fig. 9): (i) Kurz and Apps (1999), who first considered the impacts of forest disturbances on forest carbon balance, (ii) Chen et al. (2000b), who calculated the interactive effects of both disturbance and non-disturbance factors (climate, CO_2, N inputs, etc.), using Canada-wide average environmental conditions, i.e., spatially aggregated modeling, and (iii) the present study that derived Canada's annual forest carbon budgets on a 1 km grid, i.e., spatially explicit modeling. All three sets of results show similar patterns of carbon dynamics in the last

century, but the details differ considerably, particularly for the last two decades. If the effects of disturbances are considered in isolation (superimposed on the balance of stand-level growth, mortality and decomposition), the analysis by Kurz and Apps suggests that Canada's forests shifted from a carbon sink to a source around 1980, because of dramatic increases in the average carbon losses due to forest fires and insect-induced mortality. When the positive effects of non-disturbance factors (climate warming, N deposition, CO_2 fertilization) are also considered, Canada's forests appear to remain a sink during 1980–1998, albeit considerably smaller than that of the mid-20th century. The net C uptake estimated from spatially explicit modeling in the present study are similar to those of spatially aggregated modeling (Chen et al., 2000b) for the last two decades, but the historical variations differ considerably between these two sets of calculations. The regrowth of forests in areas disturbed near the end of the 19th century or the beginning of 20th century is slower in results from spatially explicit modeling than those from spatially aggregated modeling. Hence, spatially explicit modeling produces a relatively delayed increase in the
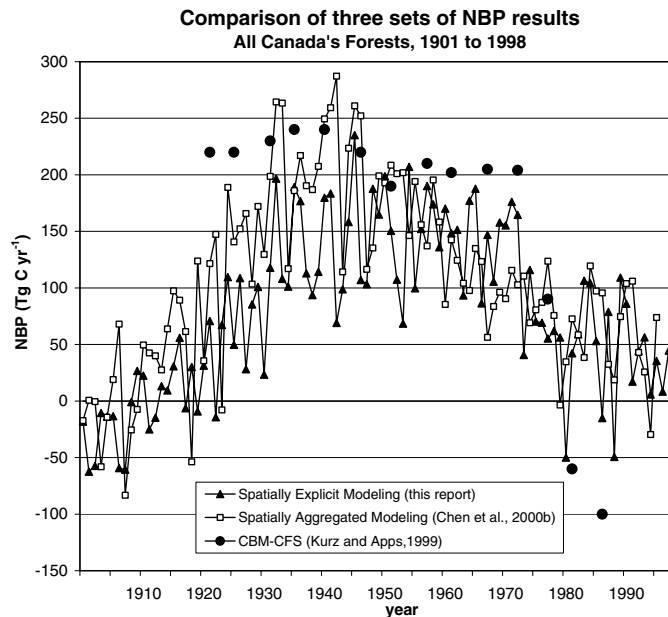
Fig. 9. Carbon balance of Canada's forests over the last century from three studies: (1) Carbon Budget Model of Canadian Forest Service (Kurz and Apps, 1999) based on national forest inventory, and accounting for changes in age structure due to disturbances; (2) Canada-wide spatially aggregated modeling of annual NBP using InTEC (Chen et al., 2000b); and (3) spatially explicit (approximately 1 km resolution) modeling of this study.

sink size toward the middle of the 20th century. Averaged over the last century, the sink magnitude from the spatially explicit modeling is 21% smaller than that from spatially aggregated modeling (Chen et al., 2000b). The main reasons are: (i) temperature increases were greater at higher latitudes, where NPP is lower than the average, causing a smaller positive response to temperature increase, but heterotrophic respiration is relatively more sensitive to temperature increase; and (ii) forest regrowth at higher latitudes is slower, so the negative effects of disturbance are more persistent than the Canada-mean conditions. Interannual variability in the pixel-based calculations is also larger than the Canada-mean calculations because of nonlinear effects of climate on the carbon cycle. In particular, the response of heterotrophic respiration to temperature changes is non-linear. These comparisons demonstrate significant improvements in understanding the spatial and temporal patterns of carbon sources and sinks achievable through the use of satellite and other spatial data. We believe that the statistics for Canada's forest carbon are improved through the spatial explicit NBP simulation. However, the values of NBP in a given year in individual pixels are strongly affected by the quality of available data. The use of more accurate, higher resolution forest age and biomass data would be the key towards improving the detailed spatial distribution pattern.

5. Conclusions

Through the use of remote sensing and other spatial data, annual carbon source and sink distributions in Canada's forests in the past century have been modeled. The mean distribution of these sources and sinks in the last decade (1990–1998) shows the following patterns: (1) source areas are associated with recent burns and sink areas with mid-age stands (40–100 yr old), and (2) sinks generally occur in southern boreal and temperate forests where NPP is high, while boreal forests at high latitudes are nearly carbon neutral.

The outcome of the study is an improvement in spatial resolution over the previous studies which were either based on 42 spatial units (Kurz and Apps, 1999) or treated all of Canada's forests as a spatially uniform aggregate of various cover types (Chen et al., 2002b). Uncertainties in the spatially explicit results for individual pixels remain large due to the lack of reliable spatial data, especially forest stand age in northern boreal forests. However, the value of the current work lies in its clarification of the general distribution of carbon source and sink regions resulting from the combined effects of disturbance and non-disturbance factors including higher temperature, N deposition and CO_2 fertilization.

In addition to capturing the spatial pattern, the annual estimates of NBP from the means of the 5 million 1 km^2 pixels may be more reliable than previous Canada-mean calculations of Chen et al. (2000b), although the differences were found to be relatively small. These two sets of results agree best for the period 1980–1998 in terms of net carbon balance. This agreement increases our confidence that the overall positive effects of non-disturbance factors (temperature, CO_2, N) probably outweighed the negative effects of large increases in the areas disturbed annually, making Canada's forests a small C sink in the period 1980–1998. Comparisons of modeled results with eddy covariance measurements at towers located in four forest stands indicate that the sink values from the present study may even be underestimated.

6. Acknowledgements

REFERENCES

Amiro, B. D., Chen, J. M. and Liu, J. 2000. Net primary productivity following forest fire for Canadian ecoregions. *Can. J. For. Res*. **30**, 939–947.

Amiro, B. D., Todd, J. B., Wotton, B. M., Logan, K. A., Flannigan, M. D., Stocks, B. J., Mason, J. A., Martell, D. L. and Hirsch, K. G. 2001. Direct carbon emissions from Canadian forest fires, 1959–1999. *Can. J. For. Res*. **31**, 512–525.

Amiro, B. D. and Chen, J. M. 2003. Dating forest fire scar using SPOT-VEGETATION for Canadian ecoregions. *Can. J. For. Res*. (in press).

Arain, M. A., Black, T. A., Barr, A. G., Jarvis, P. G.,

Massheder, J. M., Verseghy, D. L. and Nesic, Z. 2002. Effects of inter-annual and seasonal climate variability on net ecosystem productivity of boreal deciduous and conifer forests. *Can. J. For. Res.* **32**, 878–891.

Battle, M., Bender, M. L., Tans, P. P., White, J. W. C., Ellis, J. T., Conway, T. and Francey, R. J. 2000. Global carbon sinks and their variability inferred from atmospheric O_2 and sigma (13) C. *Science* **287**, 2467–2470.

Black, T. A., Hartog, G., Neumann, H. H., Blanken, P. D., Yang, P. C., Russell, C., Nesic, Z., Lee, X., Chen, S. G., Staebler, R. and Novak, M. D. 1996. Annual cycles of water vapour and carbon dioxide fluxes in and above a boreal aspen forest. *Global Change Biol.* **2**, 219–229.

Bousquet, P., Peylin, P., Cias, P., Le Quere, C., Friedlingstein P. and Tans, P. P. 2000. Regional changes in carbon dioxide fluxes of land and oceans since 1980. *Science* **290**, 1342–1346.

Burrough, P. A. and McDonnell, R. A. 1998. *Principles of geographical information systems*. Oxford University Press. New York.

Chen, J. M. and Cihlar, J., 1997. A hotspot in a simple bidirectional reflectance model for satellite applications. *J. Geogr. Res.* **102**, D22, 25907–25913.

Chen, W. J., Chen, J., Liu, J. and Cihlar, J. 2000a. Approaches for reducing uncertainties in regional forest carbon balance. *Global Biogeochem. Cycles* **14**, 827–838.

Chen, J. M., Chen, W., Liu, J. and Cihlar, J. 2000b. Annual carbon balance of Canada's forests during 1895–1996. *Global Biogeochem. Cycles* **14**, 839–850.

Chen, J. M., Pavlic, G., Brown, L., Cihlar, J., Leblanc, S. G., White, H. P., Hall, R. J., Peddle, D., King, D. J., Trofymow, J. A., Swift, E., Van der Sanden, J. and Pellikka, P. 2002a. Derivation and validation of Canada-wide leaf area index maps using ground measurements and high and moderate resolution satellite imagery. *Remote Sensing of Environment* **80**, 165–184.

Chen, W., Chen, J. M., Price, D. T. and Cihlar, J. 2002b. Effects of stand age on net primary productivity of boreal black spruce forests in Canada. *Can. J. For. Res.* **32**, 833–842.

Cihlar, J., Ly, H., Li, Z., Chen, J., Pokrant, H. and Huang, F. 1997. Multitemporal, multichannel AVHRR data sets for land biosphere studies: artifacts and corrections. *Remote Sensing of Environment* **60**, 35–57.

Cihlar, J., Xiao, Q., Chen, J. M., Beaubien, J., Fung K. and Latifovic. R. 1998. Classification by Progressive Generalization: a new automated methodology for remote sensing multichannel data. *International Journal for Remote Sensing* **19**, 2685–2704.

De Jong, R., Shields, J. A. and Sly, W. K. 1984. Estimated soil water reserves applicable to a wheat-fallow rotation for generalized soil areas mapped in southern Saskatchewan. *Can. J. Soil Sci.* **64**, 667–680.

Dignon, J. and Hameed, S. 1989. Global emissions of nitrogen and sulfur oxides from 1860–1980. *J. Air Pollut. Control Assoc.* **39**, 180–186.

Fan, S., Gloor, M., Mahlman, J., Pacala, S., Sarmiento, J., Takahashi, T. and Tans, P. 1998. A large terrestrial carbon sink in North America implied by atmospheric and oceanic corbon dioxide data and models. *Science* **282**, 442–446.

Farquhar, G. D., von Caemmerer, S. and Berry, J. A. 1980. A biochemical model of photosynthetic CO_2 assimilation in leaves of C_3 species. *Planta* **149**, 78–90.

Gholz, H. L., Wedin, D. A., Smitherman, S. M., Harmon, M. and Parton, W. J. 2000. Long-term dynamics of pine and hardwood litter in contrasting environments: toward a global model of decomposition. *Global Change Biol.* **6**, 751–765.

Goulden, M. L., Wofsy, S. C., Harden, J. W., Trumbore, S. E., Crill, P. M., Gower, S. T., Fries, T., Daube, B. C., Fan, S.-M., Sutton, D. J., Bazzaz, A. and Munger, J. W. 1998. Sensitivity of boreal forest carbon balance to soil thaw. *Science* **279**, 214–217.

Gower, S. T., Vogel, J. G., Norman, J. M., Kucharik, C. J., Steele, S. J. and Stow, T. K. 1997. Carbon distribution and aboveground net primary productivity in aspen, jack pine, and black spruce stands in Saskatchwan and Manitoba, Canada. *J. Geophys. Res.* **102D**, 29029–29041.

Gurney, K. R., Law, R. M., Denning, A. S., Rayner, P. J., Baker, D., Bousquest, P., Bruhwiler, L., Chen, Y.-H. and coauthors, 2002. Towards robust regional estimates of CO_2 sources and sinks using atmospheric transport models. *Nature* **415**, 626–630.

Houghton, R. A. 1999. The annual net flux of carbon to the atmosphere from changes in land use 1850–1990. *Tellus* **51B**, 298–313.

Humphreys, E. R., Black, T. A., Ethier, G. J., Drewitt, G. B., Spittlehouse, D. L., Jork, E.-M., Nesic, Z. and Livingston, N. J. 2002. Annual and seasonal variability of sensible and latent heat fluxes above a coastal Douglas-fir forest, British Columbia, Canada. *Agric. For. Meteorol*. (in press).

Jarvis, P. G., Massheder, J. M., Hale, S. E., Moncrieff, J. B., Rayment, M. and Scott, S. L. 1997. Seasonal variation of carbon dioxide, water and energy exchanges of a boreal black spruce forest. *J. Geophys. Res.* **102**, 28953–28966.

Kasischke, E. S., O'Neill, K. P., French, N. H. F. and Bourgeau-Chavez, L. L. 2000. Controls on patterns of biomass burning in Alaska boreal forests. In Fire, Climate Change and Carbon Cycling in the Boreal Forest, (eds. E. S. Kasischke and B. J. Stocks). Springer-Verlag, New York.

Kurze, W. A. and Apps, M. J. 1995. An analysis of carbon budgets of Canadian boreal forests. *Water, Air and Soil Pollut.* **82**, 321–331.

Kurz, W. A. and Apps, M. J. 1999. A 70-year retrospective analysis of carbon fluxes in the Canadian forest sector. *Ecol. Model.* **9**, 526–547.

Lacelle, B. 1998. Canada's soil organic carbon database. In: *Soil processes and the carbon cycle*. (eds. R. Lal, J. Kimbla, R. F. Follett and B. A. Stewart) CRC Press, Boca Raton, FL.

Liu, J., Chen, J. M., Cihlar, J. and Chen, W. 1999. Net primary productivity distribution in the BOREAS study

region from a process model driven by satellite and surface data. *J. Geophys. Res*. **104**, D22, 27735–27754.

Liu, J., Chen, J. M., Cihlar, J. and Chen, W. 2002. Net primary productivity mapped for Canada at 1–km resolution. *Global Ecol. Biogeogr*. **11**, 115–129.

Lowe, J. J., Power, K. and Gray, S. L. 1996. Canada's forest inventory 1991: the 1994 version. An addendum to Canada's forest inventory 1991. Information Report BC-X-362E. Canadian Forest Service, Pacific Forestry Centre, Victoria BC, Canada.

New, M. G., Hulme M. and Jones, P. D. 1999. Representing 20th century space-time climate variability. I: Development of a 1961–1990 mean monthly terrestrial climatology. *J. Climate* **12**, 829–856.

New, M. G., Hulme, M. and Jones, P. D. 2000. Representing 20th century space-time climate variability. II: Development of 1901–1996 monthly terrestrial climate fields. *J. Climate* **13**, 2217–2238.

Parton, W. J., Schimel, D. S., Cole, C. V. and Ojima, D. S. 1987. Analysis of factors controlling soil organic matter levels in Great plains grasslands. *Soil Sci. Soc. Am. J*. **51**, 1173–1179.

Parton, W. J., Ojima, D. S., Cole, C. V. and Schimel, D. S. 1993. A general model for soil organic matter dynamics: sensitivity to litter chemistry, texture and management. *Soil Sci. Soc. Am. J*. special publication **39**, 147–167.

Peng, C. H., Apps, M. J., Price, T. D., Nalder, I. A. and Halliwell, D. H. 1998. Simulating carbon dynamics along the boreal forest transect case study (BFTCS) in central Canada, 1. Model testing. *Global Biogeochem. Cycles* **12**, 381–392.

Penner, M., Power, K., Muhairwe, C., Tellier, R. and Wang, Y. 1997. Canada's forest biomass resources: Deriving estimates from Canada's forest inventory. Information Report BC-X-370. Canadian Forest Service, Pacific Forestry Centre, Victoria BC, Canada, 33 pp.

Rahman, H. and Dedieu, G. 1994. SMAC A simplified method for atmospheric correction of satellite measurements in the solar spectrum, *Int. J Remote Sens*. **15**, 123–143.

Ro, C., Vet, R., Ord, D. and Holloway, A. 1995. National Atmospheric Chemistry DataBase 1993. Annual Report, Acid Precipitation in Eastern Northern America, Atmospheric Environment Service, Environment Canada.

Roujean, J. L., Leroy, M. J. and Deschsmps, P. Y. 1992. A bidirectional reflectance model of the earth's surface for the correction of remote sensing data. *J. Geophys. Res*. **97**, 20455–20468.

Schimel, D. S., Braswell, B. H., Holland, E. A., Mckeown, R., Ojima, D. S., Painter, T. H., Parton, W. J. and Townsend, A. R. 1994. Climatic, edaphic, and biotic controls over carbon and turnover of carbon in soils. *Global Biogeochem. Cycles* **8**, 279–293.

Schimel, D. S., House, J. I. and coauthors, 2001. Recent patterns and mechanisms of carbon exchange by terrestrial ecosystems. *Nature* **414**, 169–172.

Schut, P., Shields, J., Tarnocai, C., Coote, D. and Marshall, I. 1994. Soil Landscapes of Canada – An Environmental Reporting Tool Canadian Conference on GIS Proceedings. June 6–10, 1994, Ottawa, 953–965.

Shannon, J. D. and Sisterson, D. L. 1992. Estimation of S and NO_{x-} N deposition for the United States and Canada, *Water, Air, and Soil Pollut*. **63**, 211–235.

Shields, J. A., Tarnocai, C., Valentine, K. W. G. and MacDonald, K. B. 1991. Soil landscapes of Canada, procedures manual and user's hand book. Agric. Can. Publ. 1868/E, Agric. Can., Ottawa, Ontario, Canada.

Stocks, B. J. 1991. The extent and impact of forest fires in northern circumpolar countries. In: *Global biomass burning: atmospheric, climatic and biopsheric implications*. (ed. J. S. Levine). MIT Press, Cambridge, MA, 197–202.

Stocks, B. J., Mason, J. A., Todd, J. B., Bosch, E. M., Wotton, B. M., Amiro, B. D., Flannigan, M. D., Hirsch, K. G., Logan, K. A., Martell, D. L. and Skinner, W. R. 2002. Large forest fires in Canada, 1959–1997. *J. Geophys. Res*. **10**, 1029/2001JD000484.

Tarnocai, C. 1996. The amount of organic carbon in various soil orders and ecological provinces in Canada. In: *Soil processes and the carbon cycle*. (eds. R. Lal, J. Kimbla, R. F. Follett and B. A. Stewart) CRC Press, Boca Raton, FL, 81–92.

Thompson, M. V., Randerson, J. T., Malmstrom, C. M. and Field, C. B. 1996. Change in net primary production and heterotrophic respiration: How much is necessary to sustain the terrestrial carbon sink?, *Global Biogeochem. Cycles* **10**, 711–726.

Trofymow. J. A. and the CIDET working group, 1998. The Canadian Intersite Decomposition Experiment (DCIDET): Project and site establishment report. Information Report BC-X-378. Canadian Forest Service, Pacific Forest Centre, Victoria, BC, Canada. 126 pp.

Walker, B. and Steffen, W. 1997. An overview of the implications of global change for natural and managed terrestrial ecosystems. *Conservation Ecol*. **1**, 2.